

7-31-2006


# Self-Assembled Composite Nano-/ Micronecklaces with SiO<sub>2</sub> Beads in Boron Strings

Hai Ni

Xiaodong Li

University of South Carolina - Columbia, [lixiao@cec.sc.edu](mailto:lixiao@cec.sc.edu)

Follow this and additional works at: [http://scholarcommons.sc.edu/emec\\_facpub](http://scholarcommons.sc.edu/emec_facpub)

 Part of the [Engineering Physics Commons](#), and the [Other Mechanical Engineering Commons](#)

## Publication Info

Published in *Applied Physics Letters*, Volume 89, Issue 5, 2006, pages #053108-

©Applied Physics Letters 2006, American Institute of Physics.

Ni, H. & Li, X. (31 July 2006). Self-Assembled Composite Nano-/Micronecklaces with SiO<sub>2</sub> Beads in Boron Strings. *Applied Physics Letters*, 89 (5), #053108. <http://dx.doi.org/10.1063/1.2245443>

This Article is brought to you for free and open access by the Mechanical Engineering, Department of at Scholar Commons. It has been accepted for inclusion in Faculty Publications by an authorized administrator of Scholar Commons. For more information, please contact [SCHOLARC@mailbox.sc.edu](mailto:SCHOLARC@mailbox.sc.edu).

## Self-assembled composite nano-/micronecklaces with Si O<sub>2</sub> beads in boron strings

Hai Ni and Xiaodong Li

Citation: [Applied Physics Letters](#) **89**, 053108 (2006); doi: 10.1063/1.2245443

View online: <http://dx.doi.org/10.1063/1.2245443>

View Table of Contents: <http://scitation.aip.org/content/aip/journal/apl/89/5?ver=pdfcov>

Published by the [AIP Publishing](#)

---

### Articles you may be interested in

[The influence of self-assembly behavior of nanoparticles on the dielectric polymer composites](#)

[AIP Advances](#) **3**, 112106 (2013); 10.1063/1.4830279

[Self-assembled growth and magnetic properties of a BiFeO<sub>3</sub>-MgFe<sub>2</sub>O<sub>4</sub> nanocomposite prepared by pulsed laser deposition](#)

[J. Appl. Phys.](#) **113**, 17B510 (2013); 10.1063/1.4795327

[Self-assembly of nanocomponents into composite structures: Derivation and simulation of Langevin equations](#)

[J. Chem. Phys.](#) **130**, 194115 (2009); 10.1063/1.3134683

[Synthesis, structure, and magnetic studies on self-assembled Bi Fe O<sub>3</sub> – Co Fe<sub>2</sub> O<sub>4</sub> nanocomposite thin films](#)

[J. Appl. Phys.](#) **103**, 07E301 (2008); 10.1063/1.2832346

[Self-assembled monolayers on ta-C surfaces: Effect of sp<sup>3</sup> /sp<sup>2</sup> ratio on adsorption rate and friction](#)


[J. Appl. Phys.](#) **93**, 8722 (2003); 10.1063/1.1540170

---

The advertisement features a 3D cutaway of a mechanical part with a colorful stress or temperature distribution. The text 'Over 600 Multiphysics Simulation Projects' is prominently displayed in white and blue. A blue button with white text says 'VIEW NOW >>'. The COMSOL logo is in the bottom right corner.

Over **600** Multiphysics  
Simulation Projects

[VIEW NOW >>](#)

 COMSOL

## Self-assembled composite nano-/micronecklaces with SiO<sub>2</sub> beads in boron strings

Hai Ni and Xiaodong Li<sup>a)</sup>

Department of Mechanical Engineering, University of South Carolina, 300 Main Street, Columbia, South Carolina 29208

(Received 4 April 2006; accepted 28 June 2006; published online 31 July 2006)

Nano-/micronecklaces with SiO<sub>2</sub> beads in boron strings were synthesized by simply sublimating the desired powders in a sealed quartz tube at high temperature. The boron strings have a rectangular cross section with width varying from 80 to 1000 nm while the SiO<sub>2</sub> beads bear either spindle or spherical shape with a size ranging from 100 nm to 5 μm. The spacing between the SiO<sub>2</sub> beads is uniform in each boron string. Both the boron strings and the SiO<sub>2</sub> beads are amorphous and free of defects. The supersaturated vapors of silicon and oxygen induced the SiO<sub>2</sub> bead formation. © 2006 American Institute of Physics. [DOI: 10.1063/1.2245443]

As structural and/or functional building blocks, one-dimensional (1D) nanostructures with intricate morphologies and multifunctionalities play an important role in constructing nano-/microscale devices, such as nano-/micro-optoelectronic devices. However, for most materials systems, direct synthesis of their 1D nanostructures with various morphologies and functionalities still remains great challenges.

Here we report distinctive necklacelike composite structures with boron nano-/microbelts as strings and SiO<sub>2</sub> as beads that were self-assembled in a chemical vapor deposition process. The strings, boron nano-/microbelts, were formed via a vapor-liquid-solid growth mechanism throughout the whole process, while the SiO<sub>2</sub> beads were generated along the strings at a certain time interval depending on the Si and O vapor pressure levels.

The marriage of boron and SiO<sub>2</sub> in the form of nano-/microstructures is expected to exhibit unique electrical and optical properties for constructing functional nano-/microdevices, and superior mechanical properties for fabricating advanced nanocomposites. Having trivalent element characterized by a short covalent radius and tendency to form strong and directional chemical bonds, boron has a high melting point around 2300 °C and high hardness close to that of diamond. Moreover, it is one of the very few elements that can be used in harsh environments, such as nuclear engineering and as a lightweight protective armor for space shuttles.<sup>1,2</sup> In particular, the recent discovery of superconducting MgB<sub>2</sub> with transition temperature ( $T_c$ ) of 39 K has triggered an intensive interest in boron.<sup>3,4</sup> Furthermore, as the other critical component, SiO<sub>2</sub> beads, of the necklacelike composite structures, SiO<sub>2</sub> has some unique and interesting blue light emission and waveguide properties. These remarkable properties render SiO<sub>2</sub> a wide application in the field of localization of light, low dimensional waveguide, and scanning near-field optical microscopy.<sup>5</sup>

The synthesis of boron-SiO<sub>2</sub> necklacelike structures was carried out in a three-zone horizontal tube furnace. Boron, silicon, and iodine powders (weight ratio 40:1:1) were mixed, compacted, loaded into a small quartz boat as source materials, together with long strips of Si (100) substrate,

sputter coated with 20 nm gold, and were positioned within a quartz tube. The quartz tube was torch sealed with a base pressure of 5 mTorr. The furnace was raised to different temperatures at 45 °C/min and held for different lengths. The morphology and chemical composition analysis of boron-SiO<sub>2</sub> necklacelike structures were performed by scanning electron microscopy (SEM, FEI Quanta 200), energy dispersive x-ray (EDX) spectroscopy, and transmission electron microscopy (TEM, Hitachi H-8000).

The as-synthesized sample was characterized by three distinctive morphologies along the strip direction, from nano-/micronecklacelike structures at low temperature, through nano-/microbelts at intermediate temperature, to nanofibrils at high temperature zone. Figure 1(a) shows a low magnification SEM image of the nano-/micronecklacelike structures, observed at the temperature re-

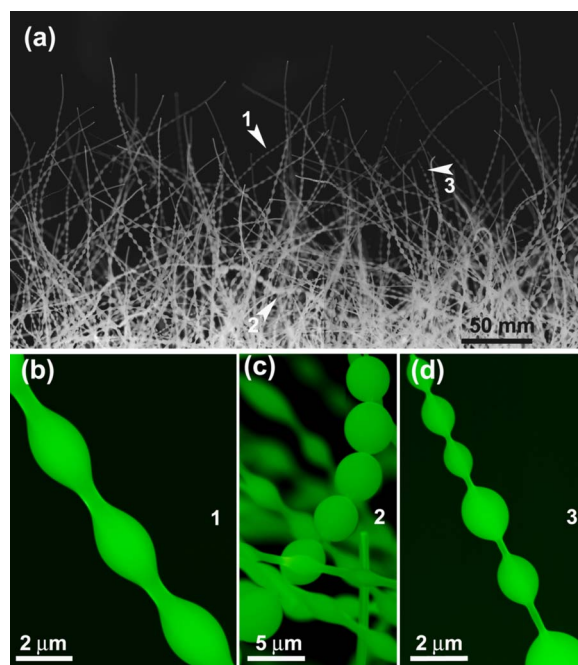


FIG. 1. (Color online) SEM images, collected under holding temperature of 1150 °C for 40 min, show (a) boron-SiO<sub>2</sub> necklacelike structures, (b) the spindle shape of SiO<sub>2</sub> beads, (c) the perfect spherical shape of SiO<sub>2</sub> beads with size up to 5 μm, and (d) necklace with beads, size from 1 to 5 μm.

<sup>a)</sup> Author to whom correspondence should be addressed; electronic mail: lixiaod@enr.sc.edu; URL: www.me.sc.edu/research/nano/

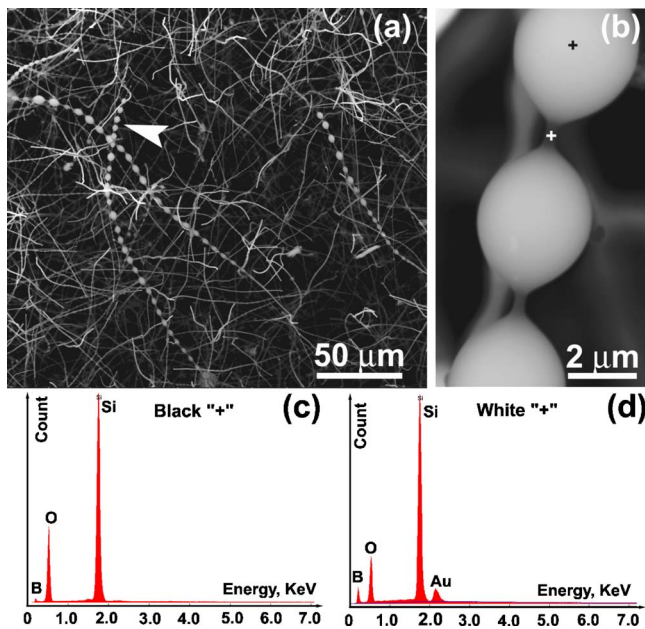


FIG. 2. (Color online) SEM images show (a) bunches of necklaces containing large beads and (b) beads with perfect spherical shape. SEM/EDX spectrum obtained from (c) the beads and (d) from the belts between the beads.

gion of 1025 °C, which is 125 °C lower than the holding temperature (1150 °C). Several runs had been performed and such necklacelike structures were 100% reproducible. Many freestanding nano-/micronecklacelike structures were observed with a couple of hundreds of micrometers long. The beads in each individual string had relatively uniform size and they were separated evenly, as illustrated in Figs. 1(b)–1(d). However, the bead size on different necklace strings was found to vary greatly from the smallest one of 100 nm to the biggest one of almost 5 μm [Figs. 1(c) and 1(d)]. The observed beads bear either spindle [Fig. 1(b)] or spherical shape [Figs. 1(c) and 1(d)], which are believed to possess minimum free energy. In some extreme cases, as shown in Figs. 2(a) and 2(b), the size of the beads can reach up to 5 μm with perfect spherical shape. No matter what the sizes and morphologies are, the bead surface is smooth and free of defects. Further extensive SEM/EDX analysis of over 40 beads indicated that the beads were close to stoichiometry composition of SiO<sub>2</sub> with O/Si atomic ratio of 2.05±0.06 [Fig. 2(c)], while the strings, going through the beads, were boron, but covered by a thin layer of SiO<sub>2</sub> [Fig. 2(d)]. Most strings had a rectangle cross section with width varying from 80 to 1000 nm. A certain amount of Si signals both in Figs. 2(c) and 2(d) originated inevitably from Si (100) substrate, resulting in the O/Si atomic ratio off the stoichiometry in both boron belt surface layer and SiO<sub>2</sub> beads.

In order to understand the SiO<sub>2</sub> bead formation mechanisms, a series of tests focusing on the growth time and growth temperature effects on the nano-/micronecklacelike structures (listed in Table I) was performed. It is interesting to point out that for the same Si(100) substrate with 20 nm gold coating and under the same maximum holding temperature of 1150 °C, when the growth time was decreased from 40 to 20 min, well formed necklacelike structures were still observed at the lowest temperature zone, but the SiO<sub>2</sub> bead size was dramatically decreased, with the biggest one smaller than 2 μm [Fig. 3(a)]. Most beads took the spindle shape [Figs. 3(b)–3(e)]. The beads with perfect spherical shape

TABLE I. Summary of the observed features under different holding temperatures and different growth times.

Growth time (min)	Holding temperature (°C)		
	1150	1050	950
40	Necklacelike structure Bead size is large	No regular bead pattern	Boron nanobelts
20	Necklacelike structure Bead size is smaller	...	...
5	Boron nanobelts	...	...

were rarely observed. When the growth time was further decreased to 5 min, only boron nanobelts were collected. On the other hand, for same growth time of 40 min but lower holding temperature of 1050 °C, although a large number of SiO<sub>2</sub> beads were observed on different boron belts, there were not enough beads on each boron belt to form regular necklacelike structures. The size of the SiO<sub>2</sub> beads varied significantly even on the same boron string. Similar to the shorter growth time, further decreasing temperature to 950 °C did not generate necklacelike structure except boron nanobelts.

As both the growth time and growth temperature have significant effects on the vapor pressure of Si (from  $2 \times 10^{-9}$  at 850 °C to  $5 \times 10^{-3}$  Pa at 1300 °C),<sup>6</sup> the SiO<sub>2</sub> bead formation on boron strings can now be understood on the basis of Si and O vapor pressure levels, as shown in the schematic diagram in Figs. 4(a)–4(e). When the synthesis temperature is high, and the growth time is short [Fig. 4(a)], gold thin film coating starts to form small islands and absorbs mainly boron atoms to initiate the growth of boron nano-/microbelts. As the growth proceeds, the vapor pressures of both Si and O continue to increase and simultaneously result in the formation of a thin layer of SiO<sub>2</sub> on the boron belt surface [Fig. 4(b)]. However, as the Si and O vapor pressures keep building up and reach a supersaturated state, which is energy unfavorable, Si and O atoms start to deposit onto the boron surface to form the first batch of SiO<sub>2</sub> beads and this process continues until the vapor pressure

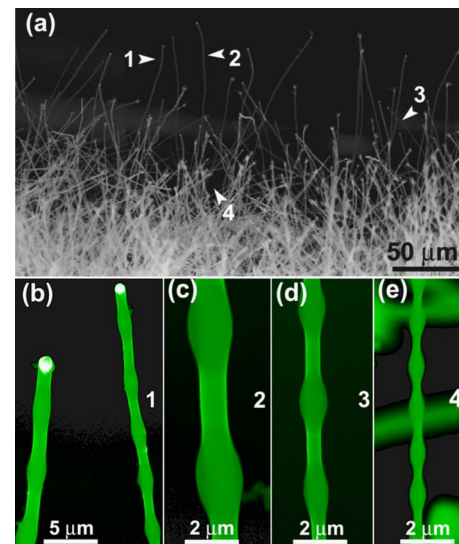


FIG. 3. (Color online) SEM images, collected under the holding temperature of 1150 °C for 20 min, show (a) boron-SiO<sub>2</sub> necklacelike structures and [(b)–(e)] the spindle shape of SiO<sub>2</sub> beads with smaller beads size.

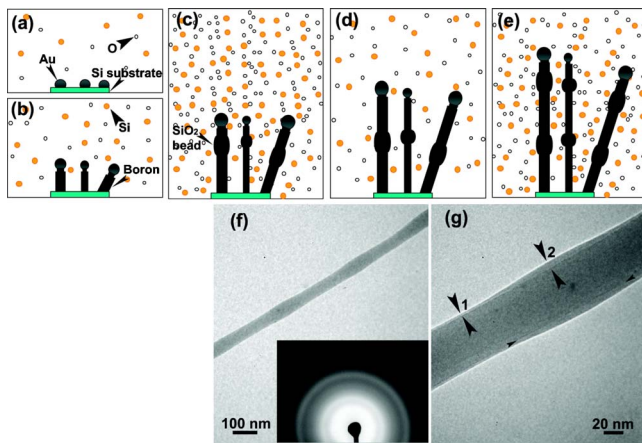


FIG. 4. (Color online) [(a)–(e)] Schematics show the formation mechanism of boron-SiO<sub>2</sub> necklacelike structure (see text for details). (f) TEM image shows the smooth and defect-free necklacelike structures. Insert is a SAD pattern. (g) High magnification TEM image shows the thickness profile of SiO<sub>2</sub> layer along one boron nanobelt.

drops to below a certain level [Figs. 4(c) and 4(d)]. Depending on the boron belt size and surface condition, the SiO<sub>2</sub> initiation sites and the final size may be different from belt to belt. As the growth time goes on, the vapor pressures of Si and O can reach the supersaturated state again and this will trigger the second batch of SiO<sub>2</sub> beads to form [Fig. 4(e)]. This cycle can occur repeatedly without interruption providing the growth time is long enough and the temperature is high enough. Neither low temperature and long growth time nor high temperature and short growth length favors this boron-SiO<sub>2</sub> necklacelike structure formation.

Another striking phenomenon is that once the SiO<sub>2</sub> beads form, their morphology maintains relatively unchanged, but the SiO<sub>2</sub> beads experience continuous growth afterwards. Due to the difference in surface tension between the boron flat surface and the curved shape of the SiO<sub>2</sub> beads, redeposition of Si and O to the formed SiO<sub>2</sub> bead surfaces, resulting in the bead size increase, is much more difficult than that on the formed fresh boron flat surfaces. Thus, as the length of boron belts extends, more and more Si and O atoms condense to form fresh embryonic droplets or nuclei on lately grown boron belt surfaces. Eventually, a long necklacelike structure is generated. According to the classical nucleation theory,<sup>7</sup> the size and ultimate morphology of the beads mainly depend on the total free energy of the SiO<sub>2</sub> beads. This energy  $W(n)$  usually consists of two items: a positive surface free energy and a negative bulk free energy difference between the supersaturated vapor and the liquid, and can be expressed by the following equation (1):

$$W(n) = -nk_B T \ln S + 4\pi\sigma(3v/4\pi)^{2/3}n^{2/3}, \quad (1)$$

where  $k_B$  is the Boltzmann constant,  $T$  is the temperature,  $S$  is the supersaturation and  $S=P/P_e$ ,  $P$  is the vapor pressure and  $P_e$  is the equilibrium vapor pressure,  $\sigma$  is surface energy per unit,  $v$  is the volume per molecule in the bulk liquid, and  $n$  is number of molecules that are transferred from the vapor to the cluster.<sup>7</sup> Since a spherical object has the minimum surface free energy for the same amount of volume, the final morphology of the SiO<sub>2</sub> beads would be perfect spherical providing the proper growth condition is served. This is why

more nice-looking necklaces with perfect spherical SiO<sub>2</sub> beads were observed at high temperature and longer growth time (Fig. 1 versus Fig. 3). The reason for the formation of SiO<sub>2</sub> beads at even spacing on the string is that the beads may not reach the critical size and weight, which allow them to slide down along the boron string to form a super SiO<sub>2</sub> bead at the root of each belt, just like the water droplets behave on the lotus leaves.<sup>8</sup>

The microstructure of the as-synthesized boron-SiO<sub>2</sub> necklacelike structures is also revealed in Fig. 4. Both low and high magnification bright-field TEM images [Figs. 4(f) and 4(g)] show that the necklace surface is smooth and free of defects. The selected electron diffraction pattern [SAD, insert in Fig. 4(f)] shows diffusive ring pattern, indicating that the as-synthesized boron-SiO<sub>2</sub> necklacelike structures are amorphous in nature. Figure 4(g) also shows an important feature about the SiO<sub>2</sub> layer thickness change along the boron nanobelt. A uniform SiO<sub>2</sub> layer was observed between the beads [position 1 in Fig. 4(g)], and it increases gradually to a maximum thickness at the pinnacle of the SiO<sub>2</sub> bead [position 2 in Fig. 4(g)]. This feature also indicates that the narrow sides of the boron nano-/microbelts may be favorable sites for SiO<sub>2</sub> beads to nucleate, since they can easily anchor themselves with the belt edges.

The intriguing boron-SiO<sub>2</sub> necklacelike nano-/microstructures could have wide potential application for their interesting semiconducting (from boron) and photoluminescent (from SiO<sub>2</sub>) properties. Since SiO<sub>2</sub> has demonstrated remarkable blue light emission capability, each SiO<sub>2</sub> bead may give off blue light and the whole necklace may work like a Christmas tree light. Another promising application is making robust nanocomposite using boron-SiO<sub>2</sub> necklacelike structures as fillers, as boron is a strong and tough material with its strength next to diamond. SiO<sub>2</sub> beads may work as excellent barriers to prevent boron belts from straightly pulling out from surrounding matrix, as commonly seen in carbon nanotube strengthened nanocomposites.<sup>9</sup>

The authors thank all staffs at USC EM Center for their SEM/EDX and TEM technical supports. Financial supports from the National Science Foundation (Grant No. EPS-0296165), the ACS Petroleum Research Fund (ACS PRF 40450-AC10), and the University of South Carolina Nano-Center are highly appreciated.

<sup>1</sup>R. M. Adams, *Boron, Metallo-Boron Compounds and Boranes* (Interscience, New York, 1964), Chap. 4, pp. 233-299.

<sup>2</sup>D. Emin, *Phys. Today* **40**, 55 (1987).

<sup>3</sup>J. Nagamatsu, N. Nakagawa, T. Muranaka, Y. Zenitani, and J. Akimitsu, *Nature (London)* **410**, 63 (2001).

<sup>4</sup>R. F. Service, *Science* **291**, 2295 (2001).

<sup>5</sup>D. P. Yu, Q. L. Hang, Y. Ding, H. Z. Zhang, Z. G. Bai, J. J. Wang, Y. H. Zou, W. Qian, G. C. Xiong, and S. Q. Feng, *Appl. Phys. Lett.* **73**, 3076 (1998).

<sup>6</sup>M. E. Levinstein and S. L. Rumyantsev, *Handbook Series on Semiconductor Parameters*, edited by M. Levinstein, S. Rumyantsev, and M. Shur (World Scientific, London, 1996), Vol. 1, pp. 1-32.

<sup>7</sup>F. F. Abraham, *Homogeneous Nucleation Theory, the Pretransition Theory of Vapor Condensation* (Academic, New York, 1974), Supplement I, pp. 225-237.

<sup>8</sup>Y. T. Cheng, D. E. Rodak, A. Angelopoulos, and T. Gacek, *Appl. Phys. Lett.* **87**, 194112 (2005).

<sup>9</sup>X. D. Li, H. S. Gao, W. A. Scrivens, D. L. Fei, X. X. Xu, M. A. Sutton, A. P. Reynolds, and M. L. Myrick, *Nanotechnology* **15**, 1416 (2004).